

Functional simulation model of the axial flux permanent magnet generator

MAREK GOŁĘBIOWSKI, ANDRZEJ SMOLEŃ, LESŁAW GOŁĘBIOWSKI, DAMIAN MAZUR

*Rzeszow University of Technology, The Faculty of Electrical and Computer Engineering
e-mail: {golebiye/mazur}@prz.edu.pl*

(Received: 21.06.2018, revised: 30.08.2018)

Abstract: The paper discusses in detail the construction of the Core Less Axial Flux Permanent Magnet generator simulation model. The model has been prepared in such a way that full compatibility with the elements of the SimPowerSystem library of the Matlab/Simulink package is preserved, which allows easy use of the presented simulation model for testing the work of the generator as part of a larger system. The parameters used in the model come from the MES 3D calculations performed in the Ansys/Maxwell software, for a machine prototype with a rated power of 2.8 kW, which was then used to experimentally verify the correct operation of the presented model of machine.

Key words: axial flux generator, circuit model, Simulink

1. Introduction

Machines with axial magnetic field flow, with permanent magnets, are characterized by a very large ratio of diameter to axial length. Due to the features of geometry desired in many applications and the simple construction of Axial Flux Permanent Magnet machines, they are increasingly used. This type of machines are more and more frequently used for generator work with wind turbine assemblies, mainly of small and medium powers. This situation creates the need to conduct simulation tests for machines of this type as an element of more complex energy systems. The generator model in the Matlab/Simulink program was made in such a way that it was compatible with elements of the SimPowerSystems library. This approach makes it easier to simulate generator operation under different conditions. It is possible to use ready-made elements of the library, thanks to which it is easy to simulate the work of the generator with various types of load or in a system with various types of power converters. This allows simulation testing of many variants of the control strategies of these converters. The generator model described can also easily be coupled with a turbine model, thanks to which a full turbine-generator-converter system will be simulated.

2. Description of the generator simulation model

The generator parameters determined in the field calculations were used to build a circuitual model used to simulate the dynamics of the generator. The investigated generator has 2.8 kW rated power at 300 rpm. In the basic model version the equations take the form of (1), (2) and (3).

$$\mathbf{u}_f = \mathbf{R} \cdot \mathbf{i}_f + \mathbf{L} \cdot \frac{d}{dt} \mathbf{i}_f + \frac{d}{dt} \theta \cdot \frac{\partial}{\partial \theta} \boldsymbol{\psi}_f, \quad (1)$$

$$m_e = \mathbf{i}'_f \cdot \boldsymbol{\psi}_f, \quad (2)$$

$$J \frac{d^2}{dt^2} \theta = m_e + m_o - \frac{d}{dt} \theta \cdot D, \quad (3)$$

where:

\mathbf{u}_f is the vector of phase voltages $\mathbf{u}_f = [u_A; u_B; u_C]$,

\mathbf{i}_f is the vector of phase currents $\mathbf{i}_f = [i_A; i_B; i_C]$,

$\boldsymbol{\psi}_f$ is the vector of magnetic fluxes of magnets coupled with phases $\boldsymbol{\psi}_f = [\psi_A; \psi_B; \psi_C]$,

\mathbf{R} is the diagonal matrix of resistance of phase windings $\mathbf{R} = [R_A, 0, 0; 0, R_B, 0; 0, 0, R_C]$,

\mathbf{L} is the phase winding inductance matrix $\mathbf{L} = [L_A, L_{AB}, L_{AC}; L_{BA}, L_B, L_{BC}; L_{CA}, L_{CB}, L_C]$,

θ is the rotation angle of the generator,

m_e is the electromagnetic moment produced by the generator,

m_o is the load moment,

D is the friction coefficient,

J is the inertia moment.

Equation (1) describes the generator's electrical substitute circuit, Equation (2) is an expression for electromagnetic torque, while (3) is a mechanical equation.

Figure 1 shows the mask of an axial flux generator model working on a three-phase RLC load connected in a star.

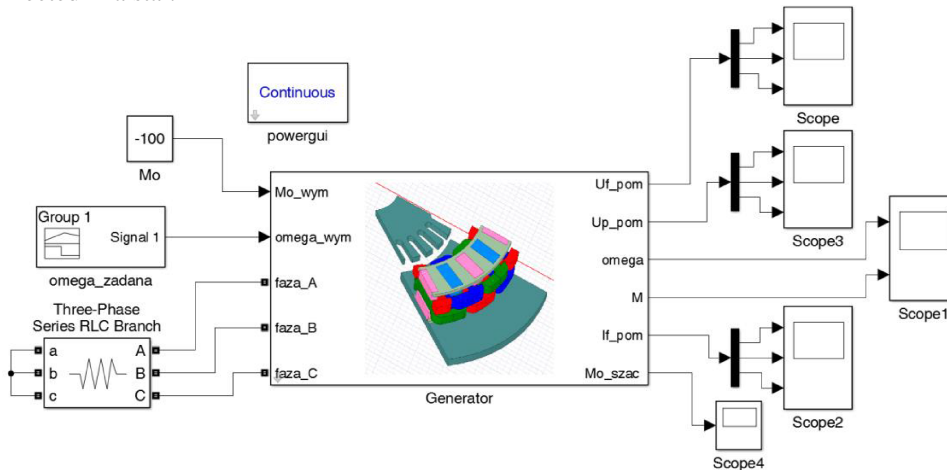


Fig. 1. Mask of a axial flux generator model working on a three-phase RLC load

Terminals labeled phase_A, phase_B and phase_C are compatible with elements of the SimPowerSystems/SimScape library. The model can work in two modes of mechanical input.

The set value can be the generator rotational speed or load moment. The corresponding input is active depending on the selection of the operating mode. In addition, the model provides measurements of phase currents as well as phase and phase-to-phase voltages, the value of the angular velocity ω , the electromagnetic moment generated by the generator m and the estimated load moment as the outputs. The last value makes sense when the generator model works in the mode with the set speed. Figure 2 shows the whole model hidden under the mask presented. The functional parts of diagram shown in Figure 2 are presented in details in Figures 3–7.

The diagram shown in Figure 3 implements electrical Equation (1). This part of the diagram is built using elements of the SimPowerSystems library, thanks to which the model maintains compatibility with elements of this library. The Mutual Inductance block is responsible for the voltage drop on the resistances and the inductance system of the coupled generator windings. The controlled voltage sources EMF A, EMF B and EMF C are responsible for the induced generator voltage described in the expression:

$$\frac{d}{dt}\theta \cdot \frac{\partial}{\partial\theta}\psi_f,$$

in Equation (1). The current measurement blocks provide the values of the phase currents necessary to determine the electromagnetic torque from Equation (2).

The values of the derivative of the permanent magnet flux coupled with the windings in the function of the rotation angle: $d\psi_A$, $d\psi_B$ and $d\psi_C$, necessary to control the voltage sources from Figure 3, are determined by the diagram shown in Figure 4.

The values of derivatives of fluxes coupled to windings come from the interpolation of the results of field calculations. This interpolation occurs in lookup table blocks. The input of these blocks is reduced to the first period of the theta mechanical angle value calculated as an integral of the omega angular velocity.

The block diagram shown in Figure 5 is responsible for determining the value of the electromagnetic torque from Equation (2).

The upper part of the diagram shown in Figure 6 is responsible for the implementation of mechanical Equation (3). The value of the speed resulting from this equation is taken into account when the model is operating in the mode with the preset torque M_{o_wym} . In the case of working with a preset speed of ω_{wym} , the speed value determined from Equation (3) is ignored. The position of the Switch determines the operating mode. When working in the mode with the specified rotational speed, the value of the load torque must be estimated (based on Equation (3)). The fragment of the generator model responsible for this task is shown in Figure 7.

As field calculations showed, the coefficients of internal and mutual inductance in the tested generator show variability as a function of the angle of rotation. In order to include this fact in the simulation, the model from Figure 2 needs to be modified. This modification consists in replacing the Mutual Inductance block responsible for the voltage drop across the resistances and the inductance system of the coupled phase windings from Equation (1), by the diagram that takes into account the dependence of the inductance factors on the angle of rotation maintaining compatibility with elements of the SimPowerSystems library.

The voltage drop on the system of generator's coupled inductances, variable in a function of the rotation angle, is described by Equation (4):

$$\mathbf{u}_L = \frac{d}{dt}\{\mathbf{L}(\theta) \cdot \mathbf{i}_f\}, \quad (4)$$

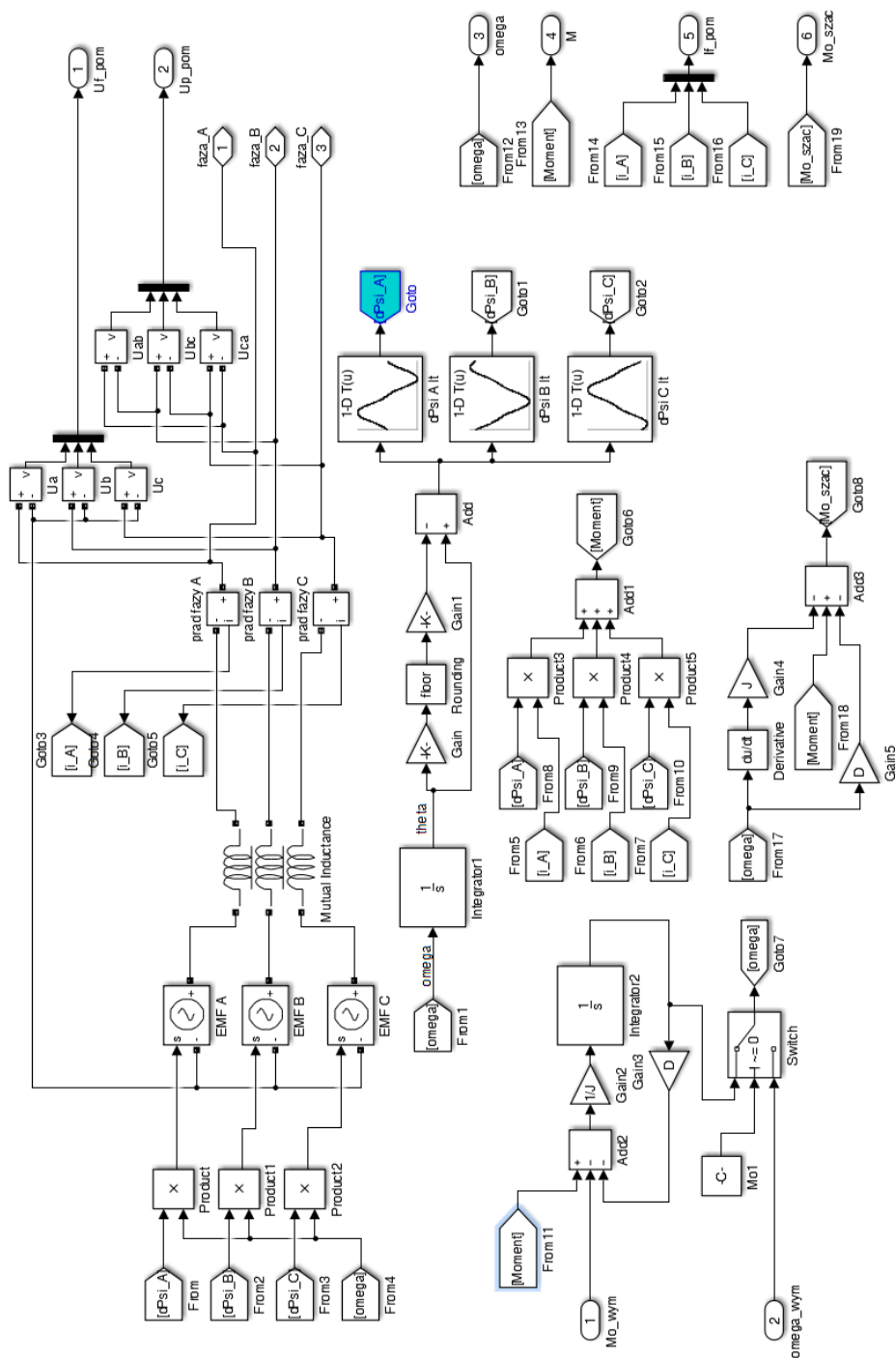


Fig. 2. Block diagram of the generator model

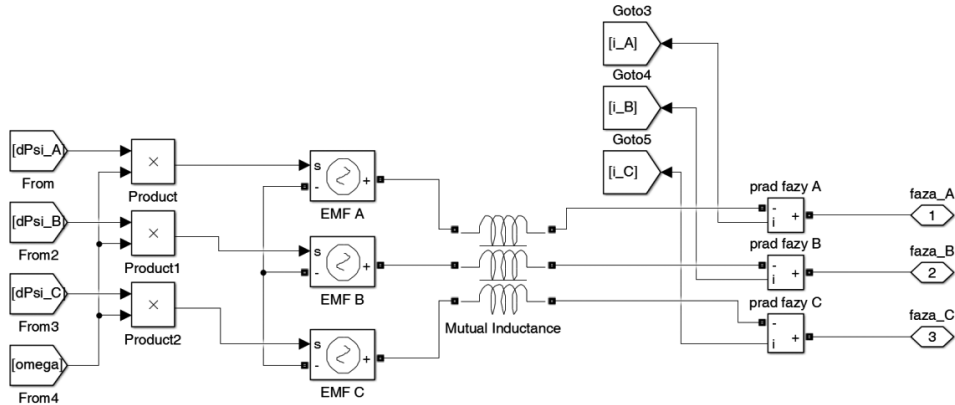


Fig. 3. Part of the diagram in Figure 2 responsible for the implementation of electrical Equation (1)

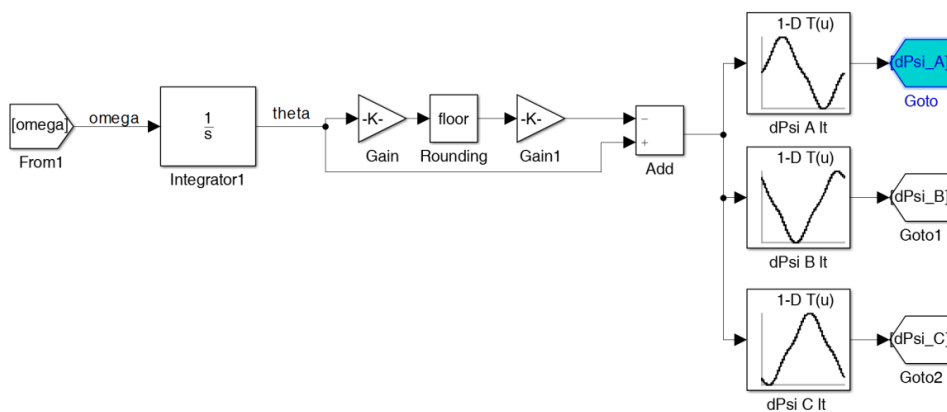


Fig. 4. Part of the diagram from Figure 2 responsible for determining the value of the derivative of the flux coupled with windings

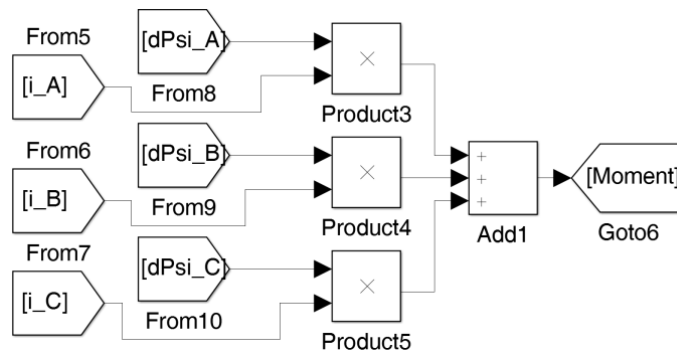


Fig. 5. The part of the diagram in Figure 2 responsible for determining the generator's electromagnetic torque

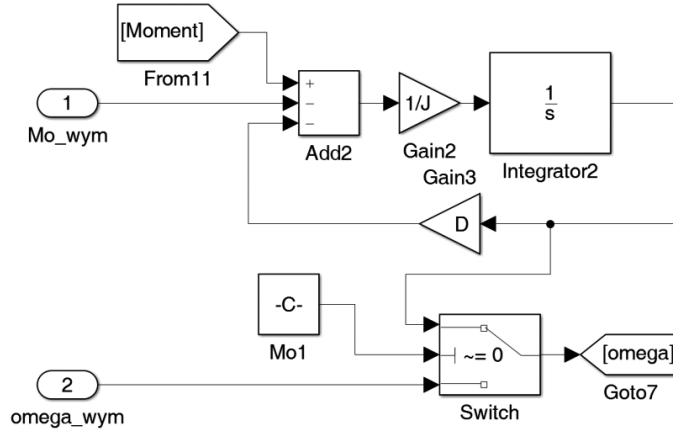


Fig. 6. The part of the diagram from Figure 2 responsible for the implementation of mechanical Equation (3) and selection of the model's operating mode

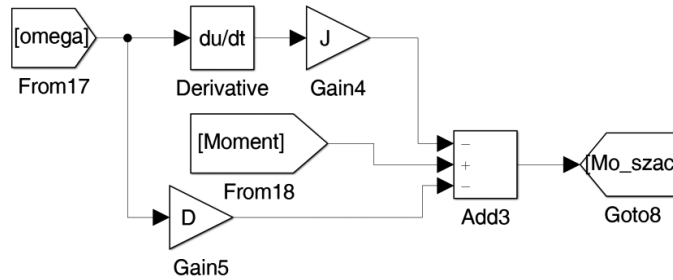


Fig. 7. The part of the diagram from Figure 2 responsible for estimating the load torque

where:

\mathbf{u}_L is the vector of voltage on inductances of generator windings $\mathbf{u}_L = [u_{L_A}; u_{L_B}; u_{L_C}]$,

$\mathbf{L}(\theta)$ is the the matrix of inductances of phase windings, variable in a function of the angle of rotation θ ,

\mathbf{i}_f is the vector of phase currents $\mathbf{i}_f = [i_A; i_B; i_C]$.

In order to model the variable inductance of the generator using elements from the SimPowerSystems library, Equation (4) transformed in the integral version was used. This equation takes the form of (5):

$$\mathbf{i}_f = \mathbf{L}(\theta)^{-1} \cdot \int_0^t \mathbf{u}_L dt. \tag{5}$$

The block diagram responsible for taking into account the variation of inductance coefficients as a function of generator rotation angle, replacing the Mutual Inductance block from Figure 2, is shown in Figure 8. The diagram in the upper part contains three models of inductance and resistance of phase windings. The phase_A winding model is shown in Figure 9. The diagram is

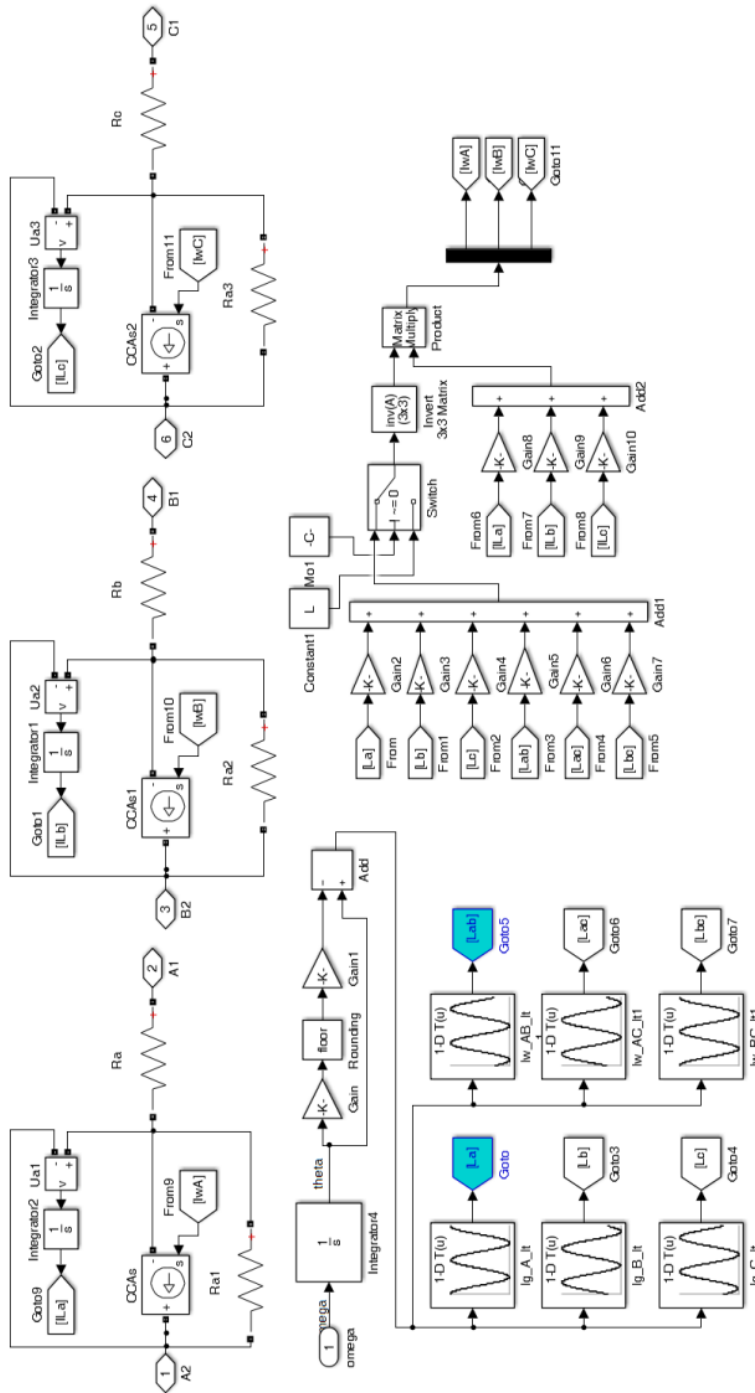


Fig. 8. Block diagram responsible for taking into account variation of inductance coefficients as a function of generator rotation angle

implemented using elements of the SimPowerSystems library. Resistance R_a is the phase winding resistance. The voltage measurement block U_{a1} measures the voltage on the inductance, which after integration in the integrator block gives the value of the integral necessary to determine the winding current from Equation (5). This value, in turn, is used to drive the current source $CCAs$ which forced the winding current. Such use of controlled current sources in a three-phase system leads to an unacceptable situation in which all loops of the system contain more than one such source. Resistor R_{a1} counteracts the described situation, its value should be chosen so that it does not affect the simulated waveforms.

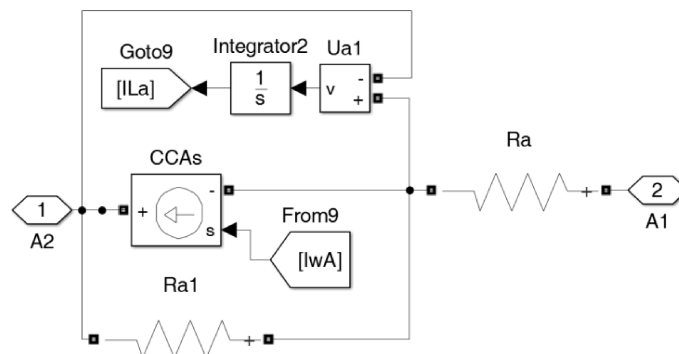


Fig. 9. A fragment of the diagram from Figure 8 modeling the inductance and resistance of phase_A winding

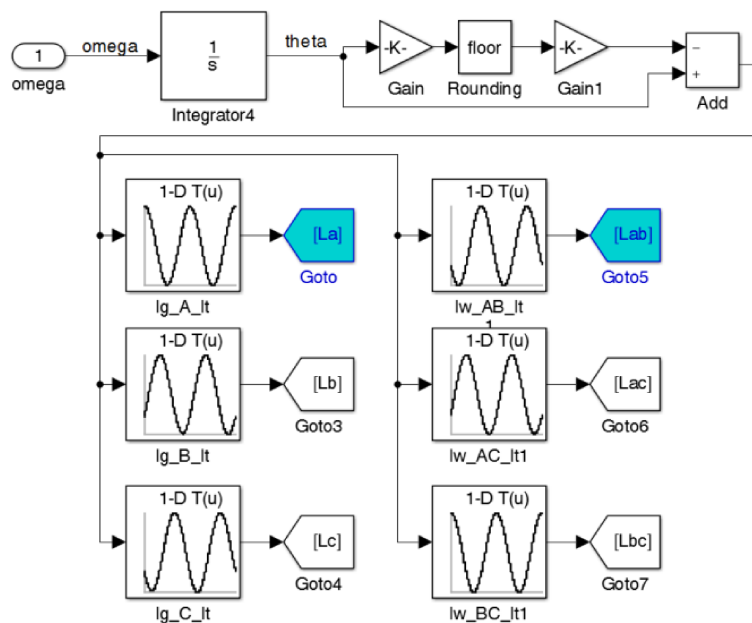


Fig. 10. A fragment of the diagram from Figure 8 responsible for generating the values of inductance coefficients

Figure 11 shows a fragment of the diagram responsible for calculating control values of current sources of phase windings in accordance with Equation (5).

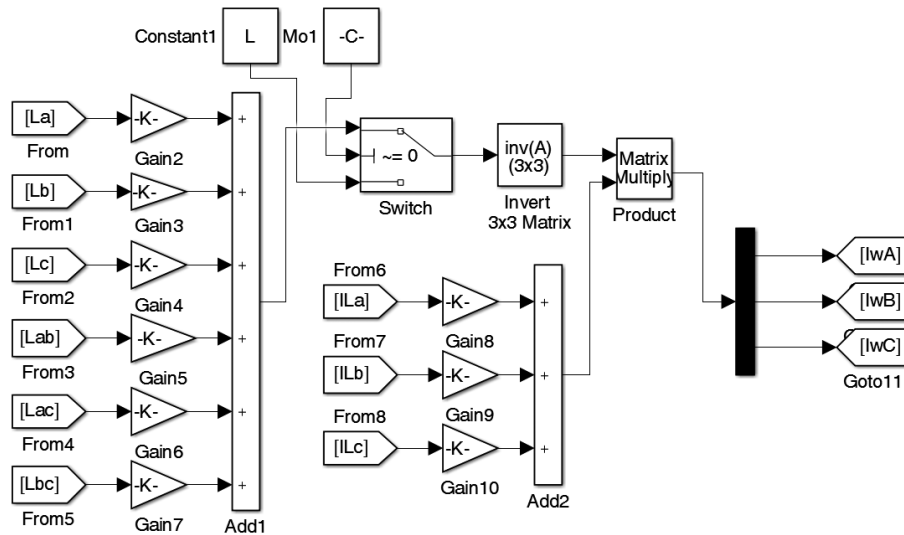


Fig. 11. A fragment of the diagram from Figure 8 responsible for implementation of calculation (5)

Experiments have shown that the variability of inductance coefficients has little effect on the waveforms in the tested generator. The proposed model will, however, enable analysis of other variants of the generator's construction characterized by greater variability of inductance coefficients as a function of the angle of rotation.

3. Experimental verification of proper function of the model

In order to verify the correctness of the constructed computational model of the axial generator described in Table 1, measurements on the generator prototype were made. Figure 12 shows the screen shot of the oscilloscope with the measurement of line voltages in the idle state of the generator for a rotational speed of 32.764 rpm.

Table 1. Waveform parameters from Figure 13

Signal	U_{RMS} [V]	U_{max} [V]	THD [%]
U_{AB} – measurement	50.23	72.6	1.43
U_{AB} – simulation	48.74	70.25	1.76
U_{BC} – measurement	49.95	72.03	1.53
U_{BC} – simulation	48.76	70.27	1.77
U_{CA} – measurement	50.33	72.64	1.49
U_{CA} – simulation	48.76	70.28	1.77

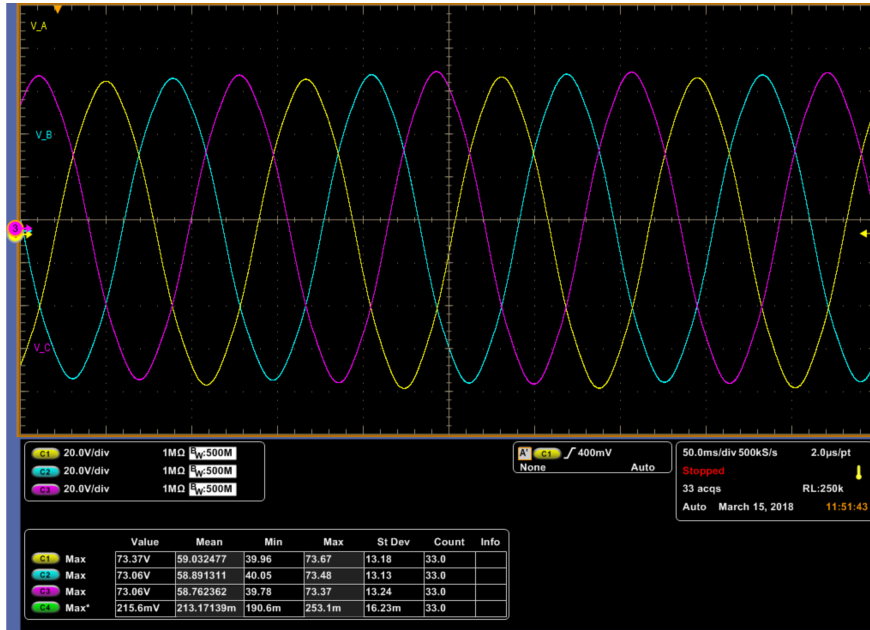


Fig. 12. Oscilloscope screen shot when measuring line voltage at idle speed for 32.764 rpm

Figure 13 shows the comparison of measurements and simulations made using the model in Figure 2. The observed waveforms show a high agreement both in shape and amplitude. The amplitude of the simulated signals is slightly smaller. Table 1 summarizes the basic parameters of the observed waveforms.

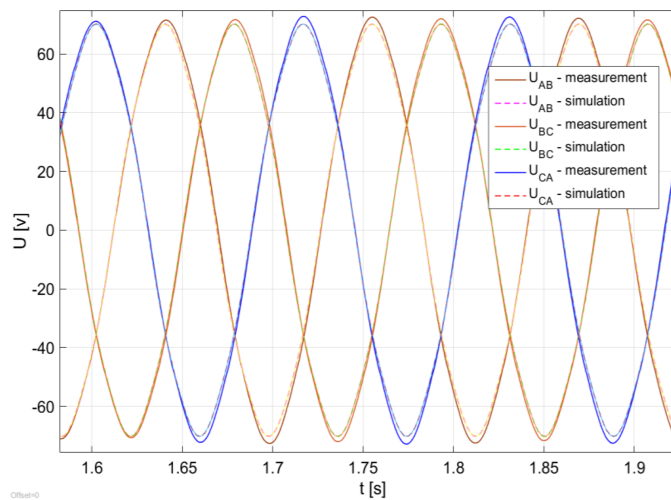


Fig. 13. Measurements and simulations results of line voltage at the output of the generator working in the idle state

4. Simulation of generator work on three phase Gretz bridge

Figure 14 shows the model of the tested generator working on a three-phase Gretz bridge. On the rectified voltage side, a capacitor with a capacity of $C = 1\,000\ \mu\text{F}$ was used. The system works on the load RL , its elements have the following values: $R_{lbc} = 110\ \Omega$, $L_{lbc} = 10\ \text{mH}$.

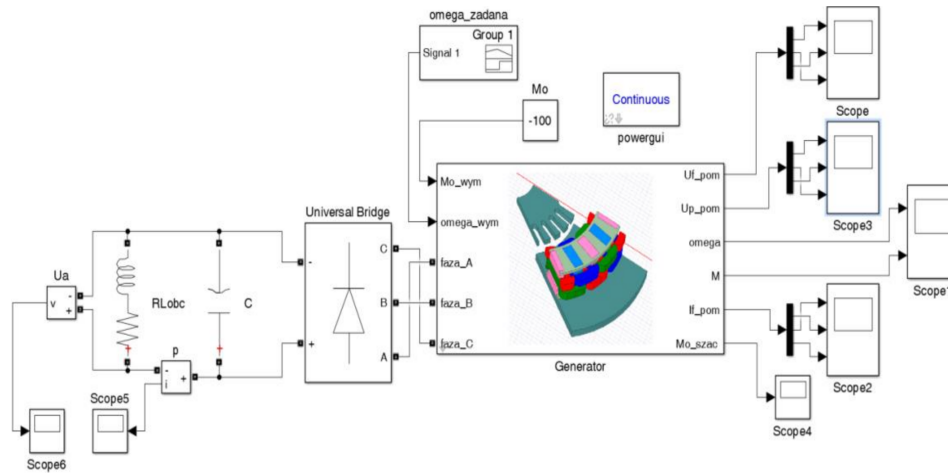


Fig. 14. A generator model working on a three-phase Gretz bridge

A system simulation was performed at a generator's rated speed of 300 rpm.

The voltage and rectified current were $U = 540\ \text{V}$ and $I_t = 5.04\ \text{A}$, with the filter capacitor able to completely remove the pulsation of the rectified voltage. In the load, the power $P = 2.794\ \text{kW}$ was dissipated.

Figures 15 show the phase voltages of the generator working on the Gretza bridge at 300 rpm.

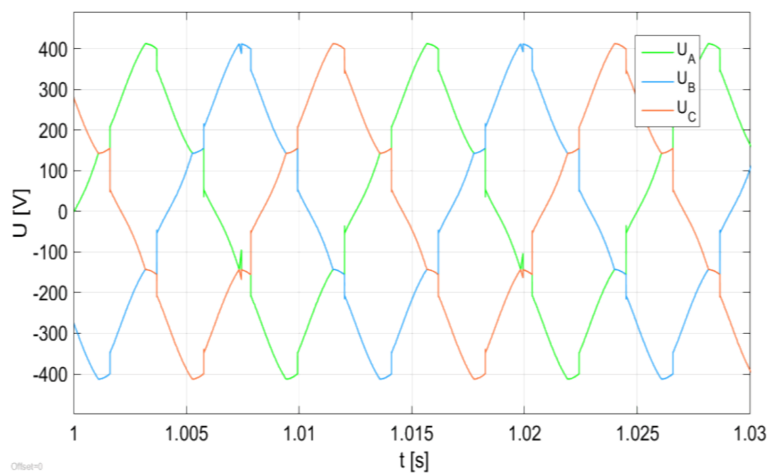


Fig. 15. The phase voltages of the generator working at Gretz bridge load with a rated speed of 300 rpm

5. Conclusions

The method of constructing the simulation model of the Core Less Axial Flux Permanent Magnet electrical machine presented in the article functions correctly. This was confirmed experimentally. The simulation model is also fully compatible with elements of the SimPowerSystem library of the Matlab/Simulink package, which, as shown in section 4, enables the efficient use of the described model to perform simulation tests of more complex systems. The discussed model was created with the aim of conducting simulation tests of the AFPM machine control strategy, working with a wind turbine, which is the subject of further work of the authors.

References

- [1] Kamper M.J., Wang R.-J., Rossus F.G., *Analysis and Performance of Axial Flux Permanent-Magnet with Air-Cored Nonoverlapping Concentrated Stator Windings*, IEEE Transactions on Industry Applications, vol. 44, no. 5, September/October (2008).
- [2] Wang R.-J., Kamper M.J., Van der Westhuizen K., Gieras J.G., *Optimal Design of Coreless Stator Axial Flux Permanent-Magnet Generator*, IEEE Transactions on Magnetics, vol. 41, no. 1, January (2005).
- [3] Wang R.-J., Kamper M.J., *Calculation of Eddy Current Loss in Axial Field Permanent-Magnet Machine With Coreless Stator*, IEEE Transactions on Energy Conversion, vol. 19, no. 3, September (2004).
- [4] Chirca M., Breban S., Oprea C.A., Radulescu M.M., *Analysis of Innovative Design Variations for Double-Sided Coreless-Stator Axial-Flux Permanent-Magnet Generator*, International Conference on Electrical Machines (ICEM) (2014), DOI: 10.1109/ICELMACH.2014.6960209.
- [5] Chan T.F., Lai L.L., *Axial flux permanent magnet synchronous generator for a direct-coupled wind turbine system*, IEEE Transactions of Energy Conversion, vol. 22, no. 1, pp. 86–94 (2007).